Fusion Engineering and Design 53 (2001) 113–121

Fusion Engineering and Design

www.elsevier.com/locate/fusengdes

High resolution ECE radiometer for electron temperature profile and fluctuation measurements on Alcator C-Mod

R. Chatterjee [a,*], P.E. Phillips [a], J. Heard [b], C. Watts [c], R. Gandy [c], A. Hubbard [d]

[a] *Fusion Research Center, The University of Texas at Austin, Austin 78712-1068, USA*
[b] *Clarion University of Pennsylvania, PA, USA*
[c] *Auburn University, USA*
[d] *Plasma Science Fusion Center, MIT, USA*

Abstract

A broadband heterodyne radiometer has been installed on Alcator C-Mod to measure second harmonic electron cyclotron emission at 234–306 GHz. The high-resolution diagnostic is now operational with 32 channels separated by < 1 cm and a frequency response of 1 MHz, measuring T_e on the low field side, for typical machine operation at $B_T = 5.4$ T. We describe the operation of the radiometer based on two novel second harmonic mixers appropriate for these high frequencies. We discuss the design and implementation of the optical system, heterodyne mixer and intermediate frequency sections. First results are presented along with the calibration of the diagnostic and comparison to other ECE diagnostics. Future plans for the diagnostic as a correlation radiometer for temperature fluctuation measurements are also discussed. © 2001 Published by Elsevier Science B.V.

Keywords: Electron cyclotron emission; Broadband; Heterodyne radiometer; Plasma temperature; High resolution

1. Introduction

Detailed knowledge of the turbulence responsible for the anomalous transport and its relation to steady state plasma parameter profiles is necessary to better understand fusion plasma confinement. Broadband heterodyne radiometry provides high spatial and temporal resolution plasma temperature measurements and is a valuable tool for understanding the evolution of advanced tokamak operation regimes. Plasma temperature measurements using correlation radiometry have been used to measure temperature fluctuations [1], study their mode structure [2] and establish their relationship to local temperature gradients [3].

A new microwave radiometer has been installed on Alcator C-Mod [4] (major radius $R = 0.67$ m, minor radius $a = 0.22$ m, $2.6 < B_T < 7.9$ T, $I_P = 0.23$–1.5 MA, $n_e = 0.24$–5.9×10^{20} m^3) to measure second harmonic electron cyclotron emission (ECE) from the low field side, and complement the existing set of Alcator C-Mod electron temperature diagnostics. This system is unique due to its high frequency (~ 300 GHz), large number of

* Corresponding author.

0920-3796/01/$ - see front matter © 2001 Published by Elsevier Science B.V.
PII: S0920-3796(00)00484-1

channels (32), high spatial resolution ($\sim 0.6 \times 2$ cm) and wide video bandwidth (1 MHz), which will allow us to make simultaneous measurements of temperature profiles and fluctuation amplitudes.

To allow complete profile measurements on the low field side with a toroidal field of 5.4 T, a standard condition for Alcator C-MOD, the frequency range of operation was chosen to be 234–306 GHz. Fig. 1 shows the range of the observed major radii for a set of toroidal fields in Alcator C-MOD. The location of channels 1 (234) to 32 (306 GHz), when measuring the second harmonic emission, is shown in groups of eight lines. Also shown are the location of the emission volumes for the same range of frequencies for the fundamental and third harmonic cyclotron emission. The vertical dash-dot line represents the major radius of the machine and the horizontal line represents the typical 5.4 T machine operation. The close spacing of the measurement points, as shown in Fig. 1 allows the use of the correlation radiometry technique developed and extensively used on TEXT-U [5–8]. We present a description of this high resolution ECE (HRECE) diagnostic hardware design and implementation, followed by a discussion of the first results of electron temperature measurements with the system.

2. Diagnostic hardware

The HRECE diagnostic has been installed on a radial port of the Alcator C-Mod tokamak. Fig. 2 shows the layout of the diagnostic in the cross-section of the tokamak, with the location of some of the second harmonic resonances for the typical case of $B_T = 5.4$ T. The diagnostic consists of a set of in-vessel collection optics that focus the ECE emission onto a set of overmoded waveguides that then carry the emission to the radio frequency (Rf) mixers. The location of the last closed flux

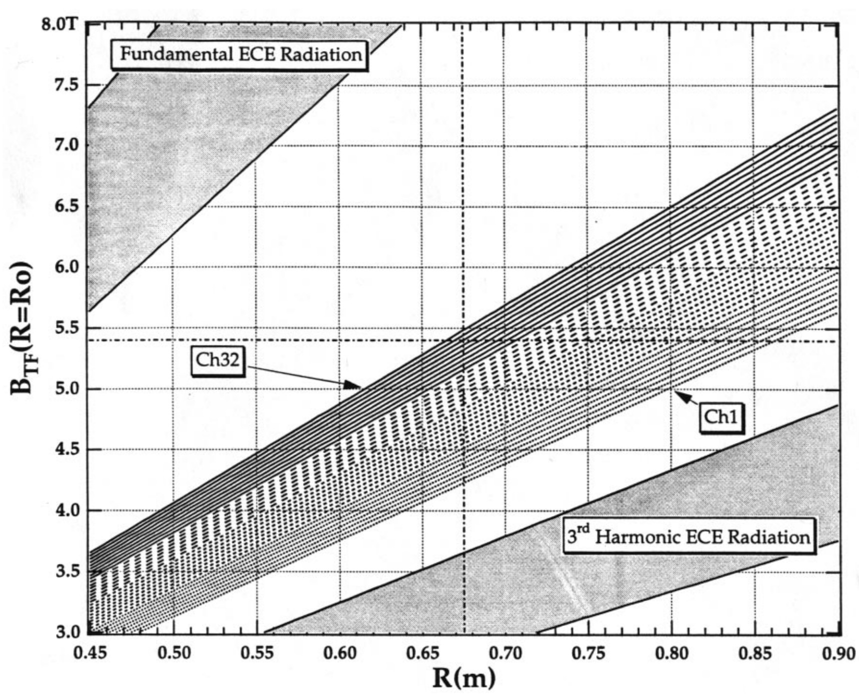

Fig. 1. Spatial location of ECE radiometer channels as a function of the toroidal field in Alcator C-Mod. The lines indicate the location of channels 1 (234) to 32 (306 GHz), when measuring the second harmonic emission for a specific toroidal field on the vertical axis. Also indicated are the fundamental and third harmonic locations for these frequencies. The vertical dashed line represents the major radius of the machine and the horizontal line represents the typical field of $B_T = 5.4$ T.

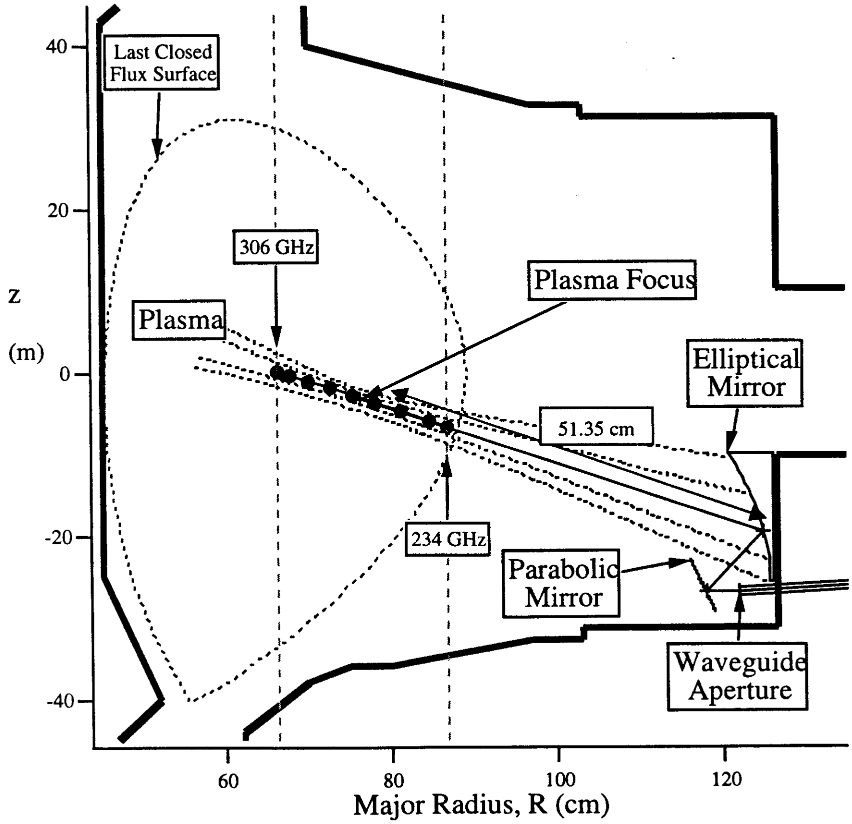

Fig. 2. Overview of the layout of the ECE radiometer diagnostic on Alcator C-Mod. The resonance positions for emission around 234 and 306 GHz is shown. Also shown are the rays used to perform Gaussian beam propagation calculations; the outer and inner rays define the $1/e^2$ and $1/e$ power levels of the beam.

surface is shown for typical conditions, from the plasma equilibrium reconstruction routinely done using EFIT [9]. A discussion of the optics, waveguide transmission system, and the construction of the radiometer follows in the rest of this section.

2.1. Optics

The optical system was designed to image a Gaussian beam waist at the plasma center onto a set of overmoded waveguides that transmit the ECE power to the radiometer. The location of other diagnostics on the same port imposed constraints on the system design. A view along the major radius was obstructed so the system observes the radiation along a beam line 15° below the major axis. The optical system consists of a set of mirrors that focus the ECE radiation in the toroidal and vertical direction. Fig. 2 shows the placement of the mirrors in the tokamak. The elliptical mirror focuses in the toroidal direction and the parabolic mirrors focus in the vertical direction. The elliptical mirror has a focal point 51.35 cm away from it surface, close to the magnetic axis of the plasma. The other focal point is at a distance of 14.26 cm from the mirror, at the aperture of the waveguide.

Cylindrical mirrors were used to allow for simpler design and fabrication. Fig. 3 shows the mirror set consisting of a section of an elliptical mirror and two parabolic mirrors that each feed a circular waveguide. An elliptical mirror was chosen for the primary collection mirror because of its frequency independent focusing properties (for

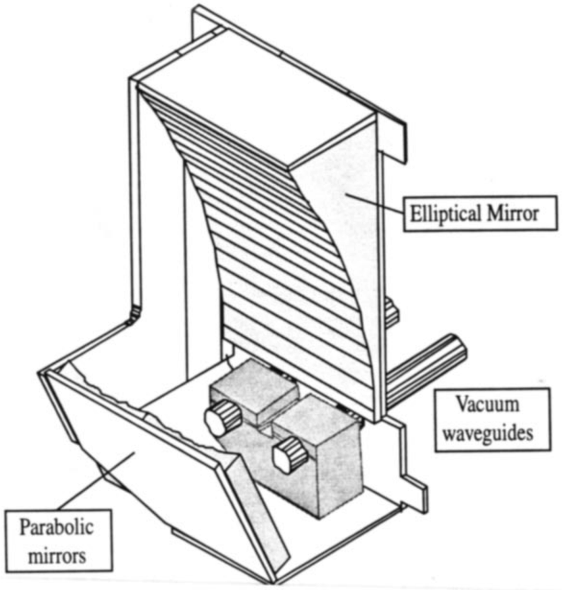

Fig. 3. Isometric view of the in-vessel optics showing the set of mirrors and vacuum waveguides. The elliptical mirror focuses vertically and the parabolic mirrors focus toroidally.

imaging between its focal points), which are critical for achieving the optimal spot size over the wide bandwidth of the system. This mirror focuses the emission vertically from a waist size of ~1.5 cm in the plasma to a waist size of ~0.17 cm at the waveguide aperture.

Two parabolic mirrors were placed between the elliptical mirror and the waveguides to provide focusing in the toroidal dimension. Each mirror is a parabolic cylindrical section with a focal length of 3.75 cm, and toroidally collimates the ECE radiation to enter separate overmoded waveguides. The mirrors couple to the internal overmoded waveguides, which are 1 cm diameter cylindrical stainless steel tube.

The mirrors and vacuum waveguides are held in position by a stainless steel frame to ensure alignment of the vacuum optics to within 0.1 mm. The vacuum breaks have been implemented with two crystalline quartz windows and the external waveguides are 1 cm diameter precision copper tubing. The measured attenuation of the entire transmission system is about 4 dB in the frequency range of interest. No mechanical displacement of the in-vessel optics or deterioration of their optical quality due to the exposure to the plasma discharges has been observed.

Fig. 4 shows the variation of the spatial resolution of the diagnostic with the major radial location of the observation sample volumes as calculated by a projection of the actual Gaussian waists to the outside midplane of the tokamak, for a typical plasma flux surface shape. The major radial resolution is ~1 cm, and the poloidal resolution is ~3 cm.

2.2. Rf system

The radiometer consists of two heterodyne receivers that convert the 234–306 GHz Rf emission from the plasma to intermediate frequencies (IF). This bandwidth was split into two 40 GHz sections set by the limits of the state-of-the art in mixers for these frequencies. Reliable sources for frequencies in excess of 200 GHz for use as local oscillators (LO) in fundamental heterodyne mixers are not available. Thus, a second harmonic mixer [10] was designed and constructed by Millitech [11] for the implementation of the radiometer. Such a harmonic mixer requires a local oscillator at half the frequency of that required for a conventional fundamental mixer. This reduces the crosstalk between the LO and the RF stages and facilitates blocking of the LO power into the antenna and optics. Another advantage is that the half-frequency LO chain requires fewer multiplier stages, thus reducing nonlinearities in the mixer response.

As shown in Fig. 5, each receiver is an integrated unit that performs a single block conversion to the IF band. Each receiver unit has an appropriate high pass filter that ensures single side-band operation of the mixers, by rejecting image frequencies below the effective LO frequencies. The high pass filters have an attenuation of 20 dB at <226 and <262 GHz and an insertion loss of 3 dB in the pass bands of >230 and >266 GHz, respectively. One heterodyne receiver has a local oscillator frequency of 115 GHz and uses a second harmonic mixer to convert the 234–270 band into 4–40 GHz. The other receiver has a second harmonic mixer with a local oscilla-

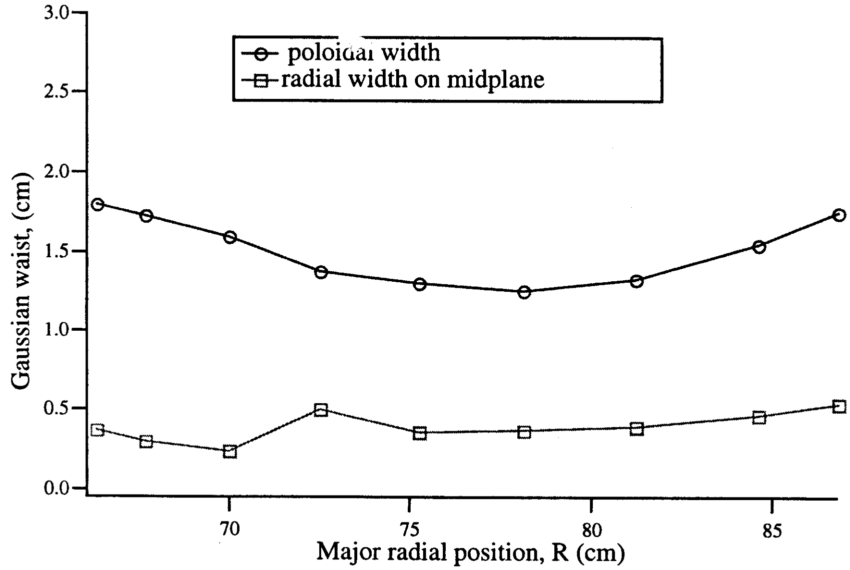

Fig. 4. Spatial resolution of the HRECE diagnostic as calculated by ray tracing. The Gaussian beam waists were projected onto the outer midplane of the tokamak to obtain the radial extent of the sample volumes.

tor frequency of 133 GHz to convert the 270–306 GHz band into 4–40 GHz. The mixer blocks have a net RF to IF gain of 10 dB, and employ an anti-parallel diode pair configuration to enhance the second harmonic mixing efficiency and eliminate the fundamental mixing response. A reliable and rugged mixer structure using planar technology, as compared with conventional whisker-contacted Schottky diode structures, fed by an integrated diagonal feed horn structure coupled to a fundamental WR-4 waveguide machined into the mixer block. The 234–270 GHz mixer has a single side-band (SSB) noise figure of 20–22 dB and a SSB conversion gain of 3–7 dB, while the 270–306 GHz mixer has a SSB noise figure of 19–30 dB and a SSB conversion gain of 0–8 dB. Integrated MMIC based IF amplifiers in the 2–50 GHz range were used to boost the signal levels, before transmission on a low-loss co-axial cable to the IF stages. The noise temperature of the entire system is set by these receivers and has been measured to be less than 10 eV.

2.3. Intermediate frequency system

The IF system was designed to be built as four modular sections using identical commercial components to reduce the complexity and cost per channel of the diagnostic. Each 40 GHz IF band was split at 22 GHz with the upper half shifted down to 4–22 GHz so that economical 22 GHz bandwidth IF components could be used. The down conversion was performed by a single block conversion using high side injection at 44 GHz, as shown in Fig. 5. The use of the 44 GHz LO for the mixer prevents contamination of the IF signals (from an LO in the 0–22 GHz band) and allows a single side-band conversion to be done without the use of additional filters. The RF–IF isolation and the harmonic conversion efficiency of these second conversion mixers are at least − 20 dB.

Each of the four 22 GHz IF signals is amplified in the IF sections with a net gain of 20–50 dB depending on the losses in the signal path. This signal is then split into eight channels by an eight-way power divider. Each channel is then filtered with band-pass filters whose center frequency is determined by dividing the 4–22 GHz band in eight equal bands. The filters have a bandwidth of 1.5 GHz (third order Chebyshev, 0.1 dB ripple) with a stop band rejection of at

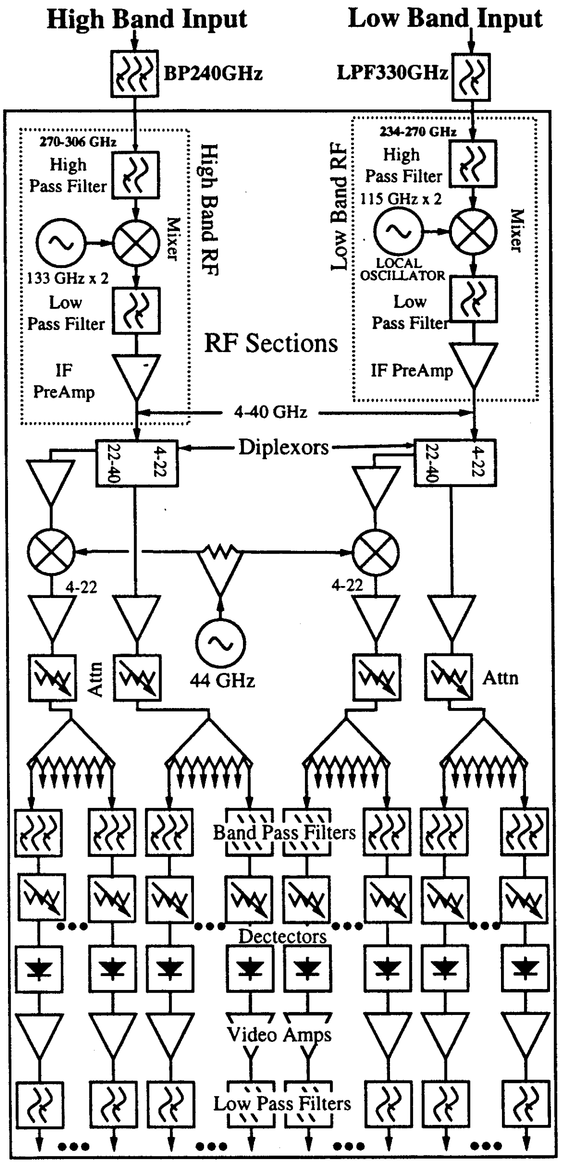

Fig. 5. Schematic of the RF and IF sections of the HRECE diagnostic. Two heterodyne mixers are used to cover the 80 GHz bandwidth. Each 40 GHz bandwidth is divided at 22 GHz into two bands; each band is divided into eight channels of equal bandwidth, detected, amplified and digitized.

least 30 dB within 0–22 GHz. Each channel is detected using a commercial 22 GHz bandwidth square-law detector with 2 V mW^{-1} responsivity. The output of the detector is amplified by a video amplifier with a 1 MHz response and digitized. The wideband video amplifiers were developed at the University of Texas to reduce the cost of the IF section. Two sets of CAMAC based data acquisition sample the signals at 20 kHz and up to 1 MHz, respectively. The slow digitizers are used to routinely obtain T_e profile information for 1.5 s and the fast digitizers are for rapid changes such as MHD and fluctuations.

3. Results

During initial operation of the diagnostic the signals from the channels viewing the edge region of the plasma were observed to have sawteeth modulation inconsistent with other T_e measurements in that region. This was traced to contamination of the signals arising from detection of ECE radiation from other regions of the plasma by third harmonic mixing in the heterodyne re-

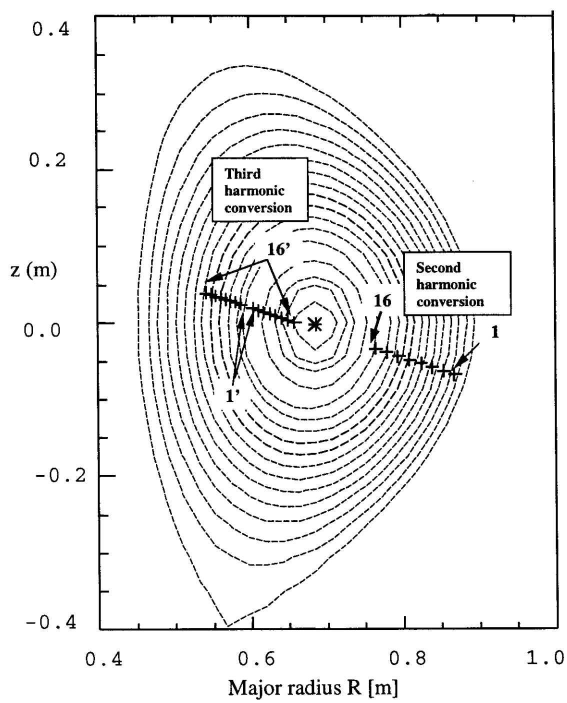

Fig. 6. Location of contamination sample volumes. The emission points detected by second harmonic conversion are shown along with the corresponding points detected by double sideband third harmonic conversion.

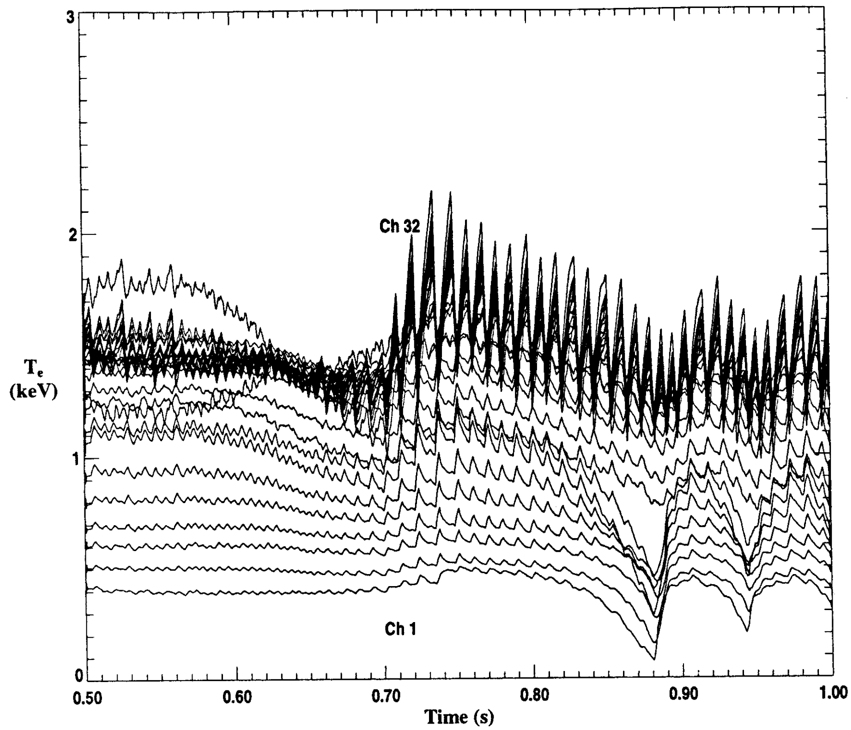

Fig. 7. Typical T_e data obtained during a discharge. Large sawteeth are observed after the injection of ICRH at 0.7 s and the apparent decrease of the temperature in the outer channels beginning at 0.8 s is due to the rise in the plasma density causing these channels to be close to cutoff.

ceiver. Thus, the output of the receiver unit operating as a second harmonic mixer with a LO of 115 GHz, was contaminated by power from frequencies at 345 ± 40 GHz. Although the efficiency of the mixer for this mode of operation is ~ 15 dB lower than the desired second harmonic mode, the contamination was significant because the emission volumes detected by third harmonic conversion are from regions of much higher temperatures, near the plasma center. Fig. 6 shows the location of the channels (1–16) in the plasma with the mixer performing second harmonic conversion, and the location of the emission volumes (1′–16′), which are detected in the same IF bandwidth by double side-band third harmonic conversion. To eliminate this contamination we have installed a multi-mesh bandpass filter [12], to block the contaminating Rf frequencies from reaching the mixer with a LO of 115 GHz, which was considered to have the most contamination. These filters have insignificant losses in the pass band and offer about 20 dB rejection in the stop band. With the bandpass filter, the signal contamination is reduced to less than 0.25%. A similar filter will be installed at the input of the other mixer unit.

Typical data obtained from all 32 channels of the HRECE diagnostic is shown during a discharge in Fig. 7, smoothed over 2.5 ms for the plot. The channels extend from channel 1 at $R_{\rm mid} = 0.837$ m (at the outer midplane) to channel 32 at $R_{\rm mid} = 0.634$ m. The inner channels clearly show modulation of the temperature due to the sawteeth instability and the inversion of the sawteeth is evident in the outer channels. The increase in the size of the sawteeth at 0.7 s is due to the injection of ion cyclotron heating power. The apparent decrease of the temperature in the outer channels beginning at 0.8 s is due to the rise in the plasma density causing these channels to be close to cutoff.

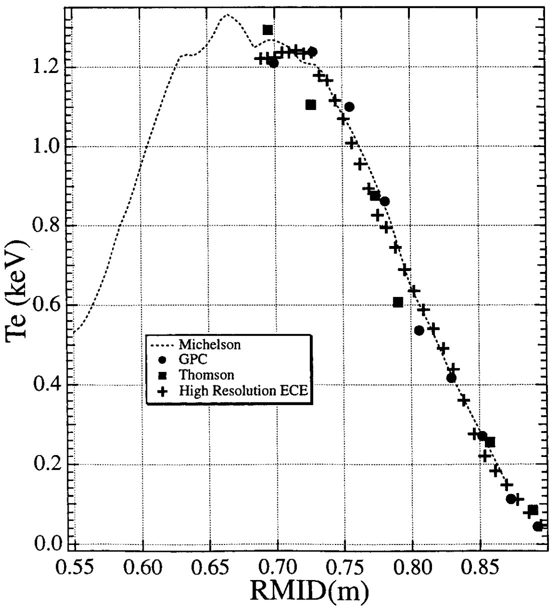

Fig. 8. T_e profile for the Ohmic phase of a discharge. Good agreement is seen between the grating polychromator, Thomson scattering, Michelson interferometer and the HRECE radiometer diagnostics.

A relative calibration of the 32 channels was performed by moving the observation locations in the plasma between adjacent channels using a small ramp in toroidal field (0.2 T), during which the change plasma parameters was negligible. Absolute temperature profiles are obtained by normalizing to the measurements of the Michelson interferometer system on Alcator C-Mod, which is absolutely calibrated. The electron temperature profiles obtained for a typical Alcator C-MOD ohmic discharge is shown in Fig. 8, along with profiles measured by the grating polycrhomator diagnostic, Thomson scattering and the Michelson interferometer. Good agreement is seen among all the diagnostics.

3.1. Temperature fluctuation measurements

Experiments are presently underway to use the diagnostic as a correlation radiometer to measure turbulent temperature fluctuations. By correlating the detected output of two channels observing non-overlapping emission frequencies from the plasma, the noise inherent in the temperature measurement is reduced to a level that allows the measurement of fluctuations. The diagnostic will be used as a correlation radiometer by cross-correlating the outputs of channels within the radial correlation length of the turbulence.

The radial extent of the plasma emission volume is related to the detection bandwidth by,

$$\Delta R = \left(\Delta\omega_{\mathrm{IF}} + \frac{\Delta\omega}{(1+\tau)}\right)\frac{R}{\omega_c}$$

where, R is the scale length of the toroidal field, ω_c the cyclotron frequency, $\Delta\omega_{\mathrm{IF}}$ the radiometer video bandwidth, and τ is the optical thickness. The resonance line width $\Delta\omega_l$ is the sum of the Doppler and relativistic broadening, and its effect on the spatial resolution is minimized by the high optical thickness (>10) in most of the plasma of Alcator C-Mod. The current set of IF filters have a bandwidth of 1.5 GHz and allow a resolution ($\Delta\omega_{\mathrm{IF}} \times R \times \omega_c$) of ~ 1 cm.

The current IF system has been designed with wide bandwidth filter to optimize the signal to noise ratio of the diagnostic for the measurement of temperature profiles. A new high resolution IF unit is being implemented with a set of IF filters with center frequencies separated by 625 kHz, bandwidth of 500 kHz, and a very large attenuation outside the band.

The expected range of sensitivity of the HRECE diagnostic to turbulence is estimated by the highest wavenumber observable without averaging over the sample volumes, which are shown in Fig. 4. The highest poloidal wavenumbers $k_\theta = \pi/3 = 1\ \mathrm{cm}^{-1}$, is close to the range expected for electron drift waves, with $k_\theta\rho_s \sim 0.1$. Although the diagnostic is inherently incapable of measuring the poloidal wavenumber spectrum because of its view, the correlation of sample volumes within the radial correlation length of the turbulence may allow the measurement of the amplitude of temperature fluctuations.

4. Conclusions

A new ECE radiometer diagnostic has been installed on Alcator C-Mod. It has an excellent combination of spatial and temporal resolution and is capable of measuring electron temperature profiles of the entire low field side of the plasma, for typical discharge conditions. The diagnostic is fully operational and is being used to routinely measure T_e profiles. A new IF section with closely spaced narrow bandwidth filters has been installed and will be used to measure T_e fluctuations.

Acknowledgements

We acknowledge valuable discussions with Dr Giuseppe Cima and Richard Chedester at Millitech. The work in this paper has been supported by D.o.E. Grant No. DE-FG03-96ER-54373.

References

[1] G. Cima, Nuovo Cimento D 16 (1994) 359.
[2] B.H. Deng, D.L. Brower, G. Cima, C.W. Dornier, N.C. Luhmann, Jr, C Watts, Phys. Plasmas 12 (1998) 4117.
[3] C. Watts, Phys. Rev. Lett. D 75 (1995) 1759.
[4] J.H. Hutchinson, R. Boivin, F. Bombarda, P. Bonoli, S. Fairfax, C. Fiore, Phys. Plasmas 1 (1994) 1511.
[5] G. Cima, R.V. Bravenec, A.J. Wootton, et al., Phys. Plasmas 2 (1995) 720–726.
[6] C. Watts, G. Cima, R.F. Gandy, et al., Rev. Sci. Instrum. 66 (1995) 451.
[7] C. Watts, R.F. Gandy, Phys. Rev. Lett. 75 (1995) 9.
[8] G. Cima, R.V.Bravenec, C. Watts, in: Seventh International Toki Conference on Plasma Physics and Controlled Nuclear Fusion, 1995.
[9] L.L. Lao, H. St. John, R.D. Stambaugh, A.G. Kellman, W. Pfeiffer, Nucl. Fusion 25 (1985) 1611.
[10] Stephen A. Maas, Microwave Mixers, Artech House, Dedham, MA, 1986.
[11] Millitech Corp., South Deerfield, MA.
[12] QMC Instruments Ltd., West Sussex, UK.